Chemical Modification of Semiconductor Surfaces by Means of Nanometric Cellulose Films

Manuel R. Vilar,*,† Sami Boufi,‡ Ana Maria Ferraria,§ and Ana Maria Botelho do Rego§

ITODYS (CNRS-Université Paris Diderot), Paris, France, Laboratoire Sciences des Matériaux et Environnement, Faculté des Sciences de Sfax, Sfax, Tunisia, and Centro de Química-Física Molecular, IST, Technical University of Lisbon, Lisbon, Portugal

Received: May 18, 2007; In Final Form: June 15, 2007

Cellulose films of nanometric thickness were produced by spin-coating on GaAs(100). Films were deposited using cellulose silylated solutions and subsequently regenerated by exposing them to vapors of hydrochloric acid. After regeneration, these films can strongly resist solvents. Modification of the film surface region was performed by immersing the regenerated cellulose films in a solution of phenyl isocyanate in dimethyl sulfoxide. A different functionalization was also successfully achieved through the interaction of the film surface with 4,4′-methylenebis(phenyl isocyanate) (MDI). Surfaces treated with MDI keep an unreacted isocyanate group and can again be modified by amines. For this purpose, 4-bromoaniline was used. All kinetics of the different molecular interactions with the cellulose film on GaAs were followed in situ using FTIRS in ATR/MIR (attenuated total reflection in multiple internal reflections) mode. Besides ATR/MIR having an analysis depth on the order of 1 μm, other surface techniques were used for analyzing these films with other probing depths such as X-ray photoelectron spectroscopy with ∼10 nm and high-resolution electron energy loss spectroscopy with ∼1 nm in the impact regime. The set of methods presented here represents a quite adequate way to study the surface chemistry of cellulose films and the procedures for their functionalization.

Introduction

Surface modification for semiconductors is an up to date subject of large interest. Particularly, functionalization of semiconductor surfaces through organic compounds is emerging as a very important domain in the development of hybrid materials for electronic devices. The methods used to incorporate chemical functions with specific properties, especially chemical recognition, have also undergone some important improvements in recent years. However, chemical grafting of organic molecules on semiconductors is strongly limited by the surface reactivity of the substrates. One of the reasons is that semiconductors are mostly covered by oxide layers and polluted by environmental contamination. To enhance the surface reactivity, cleaning and etching procedures are always obligatory. Etching, in particular, can render hydroxyl groups available, somehow improving the reactivity of the surface. In fact, the presence of hydroxyl groups so exposed on the oxide layer can now and then help to solve this problem. However, in many cases the reactivity is still poor to graft the sensing molecules. We introduce through this study a novel method to modify semiconductor surfaces by using a well-established protocol to produce an ultrathin cellulose film on them and functionalizing it subsequently. Here, the presence of a high concentration of hydroxyl groups of the cellulose exposed in the interface strongly improves the reactivity of the semiconductor surface.

Gallium arsenide surfaces were used here. Actually, this semiconductor is an interesting component in electronic devices where a fast response is needed as, for instance, in chemical sensing. This behavior is mainly due to the high mobility of the carriers in GaAs.[1] Also, the possibility to create heterojunctions with GaAs enables the confinement of carriers near the surface, improving the sensitivity of the sensor. These are the main reasons why GaAs is in the base of the development of recent hybrid (organic−inorganic) systems.[2,3] Also, the fact that GaAs of semi-insulating type is highly transparent in, practically, the whole middle infrared region enables ATR (attenuated total reflection) elements to be used to follow the chemical reactions occurring on the surface by means of the ultrathin film of cellulose.[4]

Recently, spin coating has emerged as a method for cellulose layer preparation by using a (trimethylsilyl)cellulose (TMSC) derivative as the starting material to prepare the organic solutions. Subsequently, cellulose can be regenerated by a smooth acid hydrolysis by exposing the film surface to hydrochloric acid vapors.[5−9] However, the application of these model surfaces has been limited to study the adsorption of a polyelectrolyte on the cellulose substrate[10,11] and has never been explored to study chemical reactions prone to occur on the cellulose backbone. In this study, cellulose films with nanometric thicknesses were produced and used as a novel way to functionalize GaAs(100) surfaces. The possibility of creating chemical architecture on these surfaces is also presented. Thanks to the particular structure of cellulose—a regular chemical structure, the presence of several hydroxyl groups with strong intra- and interchain hydrogen bonding, and a high molecular weight—cellulose ultrathin films will be very stable and extremely difficult to solubilize, once they have been formed. These cellulose layers were already reported to be an excellent means to study the physical chemistry of cellulose surfaces such as their interaction with water, the influence of light in the aging and yellowing processes of paper, and their thermal degradation.[6,7] Furthermore, new functions can also be introduced via cellulose layers regarding the rich chemistry of their OH groups.

* To whom correspondence should be addressed. E-mail: reivilar@paris7.jussieu.fr.
† ITODYS (CNRS-Université Denis Diderot).
‡ Faculté des Sciences de Sfax.
§ Technical University of Lisbon.

10.1021/jp073850a CCC: $37.00
Published on Web 08/07/2007

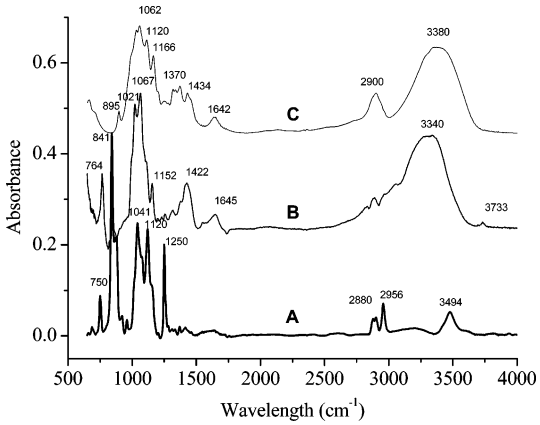

Figure 1. Comparison of ATR/MIR spectra of a TMSC spin-coated film before (A) and after (B) hydrolysis with the transmission spectrum of pure cellulose (Avicel) dispersed in a KBr pellet (C). The main peak positions are specified.

TABLE 1: Assignment of the Major Peaks Found in ATR/MIR Spectra of a TMSC Spin-Coated Film before (A) and after (B) Hydrolysis and Those of the Transmission Spectrum of Pure Cellulose (Avicel) Dispersed in a KBr Pellet (C)

wavenumber (cm^{-1})				
A	B	C	intensity	vibration mode assignment[20−23]
750	764		m	Si−C rocking
841	841		vs	Si−C rocking
	a	895	s	γ(COC) in plane, sym stretching
	1021	a		C−O stretching + CH_2 rocking
1041			s	Si−O stretching
a	1067	1062	vs	C−O−C asym stretching
1120	a	a	s	Si−O stretching + CH_2 deformation
a	1152	1166	vs	CH and OH deformation
1250			s	sym CH_3 deformation
	1422	1434		CH_2 sym bending
	1645	1642		associated OH stretching
2880			m	asym CH_3 stretching
	2883	2900		CH_2 stretching
2956			m	sym CH_3 stretching
3494	3340	3380	m	associated OH stretching
	3733			isolated OH stretching

[a] Weak shoulder.

In this study, we show that cellulose layers can also be used for surface functionalization. This possibility opens the way to the introduction of specific functional groups and in particular those leading to new technological applications in the field of sensors and biosensors.

Actually, the chemistry of cellulose and isocyanates is well-known in both the homogeneous[12,13] and the heterogeneous[14,15] phases. Thanks to the high reactivity of the isocyanates toward species bearing hydroxyl groups, these molecules found a great interest in the field of polymer synthesis and modification. In the particular case of cellulose, a lot of work has been carried out. This development in cellulose chemistry led us to choose isocyanate molecules to carry out the modification of ultrathin cellulose films deposited on GaAs semiconductor surfaces. In fact, this study allows us to verify whether the reaction follows the same trends under homogeneous conditions in free fibers as in heterogeneous conditions on a film surface. The recourse to a bifunctional isocyanate can be an effective way to introduce new functionalities to the surface and can also be exploited for further modifications of the cellulose surface. This study demonstrates that it is possible to apply the same chemistry on the modification of nanometric films of cellulose deposited on a semiconductor substrate, keeping their integrity.

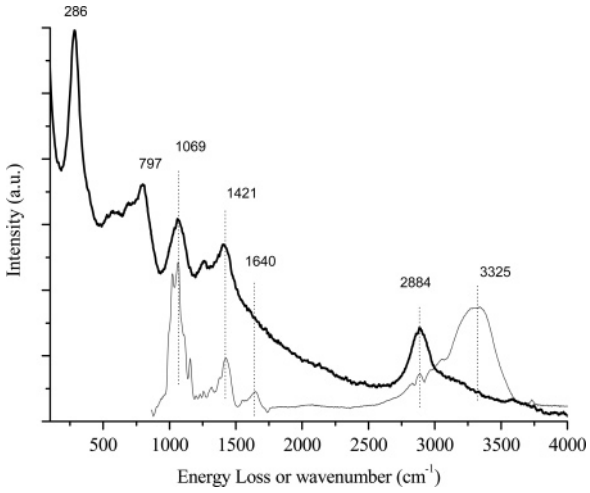

Figure 2. Comparison between ATR/MIR and HREELS (bold) spectra of a regenerated cellulose thin film on GaAs. The HREELS spectrum was recorded using incident electrons of 2.5 eV, an angle of incidence of 60°, and an angle of diffusion of 30°.

It is well-known that isocyanate interacts with the hydroxyl groups of cellulose.[15] The interaction results in the formation of a carbamate through the transformation of the NCO group. The vibrations of the NCO groups before and after the reaction with cellulose, corresponding to the isocyanate and the urethane groups, are distinct and can be followed by infrared spectroscopy in the mode of attenuated total reflection in multiple internal reflections (ATR/MIR). This feature can be used to follow the kinetics of the surface modification and the concomitant condensation reactions. In this study, different molecules were tested. First, the kinetics of the interaction of phenyl isocyanate (PI) with a cellulose surface was followed. Second, another molecule, the 4,4′-methylenebis(phenyl isocyanate) (MDI) was also used. This last molecule contains an isocyanate group in each extremity. It follows that one of the groups can chemisorb to the cellulose film whereas the other one can be used for a further chemical reaction on the surface. Due to the short lengths of the molecules used here, only one of the isocyanate groups can bind to the surface. The other isocyanate group stays free and can react afterward with a base, for instance, an amine. In this case, 4-bromoaniline (BrA) was used to derivatize the cellulose.

The study of the different molecular layers was accomplished by crossing the information obtained with different techniques such as ATR/MIR, X-ray photoelectron spectroscopy (XPS), and high-resolution electron energy loss spectroscopy (HREELS).

All the surfaces studied here were analyzed by ATR/MIR and XPS. ATR/MIR was revealed to be an ideal method to follow the kinetics of the surface modification. Following the evolution of the NCO band in the ATR/MIR spectra helped to establish the mechanism of the reaction between this functional group and the cellulose film surface. With XPS it is possible to characterize both qualitatively and quantitatively the chemical composition of the outermost layer that is within 10 nm of the film. First, HREELS spectra of a cellulose surface are presented here. HREELS sensitivity to the surface is very high, and the depth of analysis is less than 1 nm. The analysis of different depths by ARXPS (XPS with angle resolution) allows estimation of the thickness of the adsorbed organic layer. This study can also be useful to search new methods for molecular architecture through the use of cellulosic nanometric films.

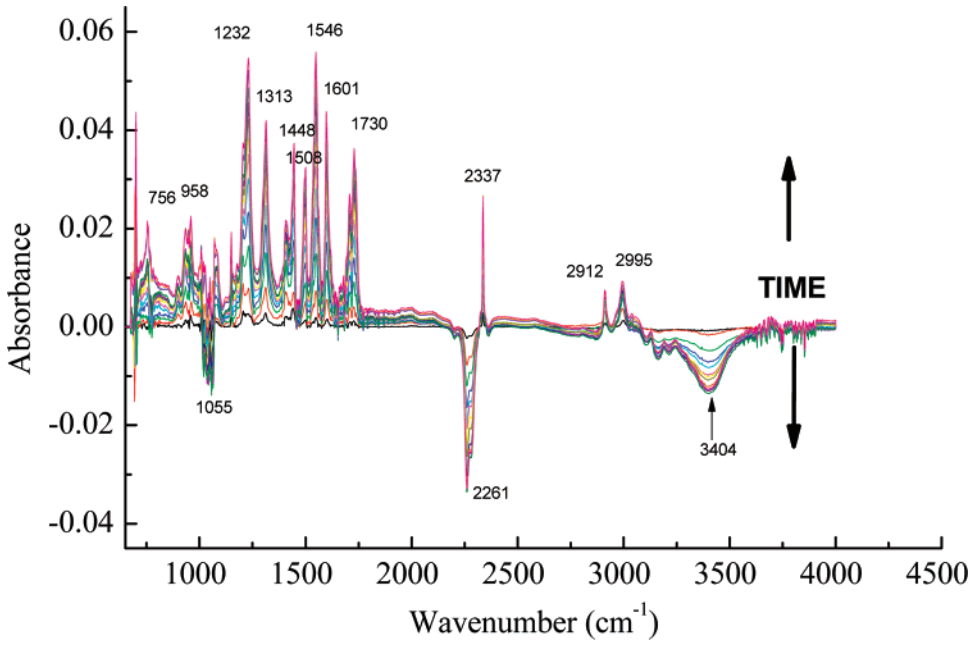

Figure 3. ATR/MIR spectra of a cellulose regenerated film in interaction with a solution of PI in DMSO recorded in situ at different times after the background recording. Arrows indicate the time evolution.

Experimental Section

Materials and Chemicals. Undoped semi-insulating single-crystal GaAs wafers with orientation (100) were acquired from Geo Semiconductors Ltd. PI with purity better than 98% from Alfa-Aesor was used as received. MDI and 4-bromoaniline (97% pure) were acquired from Aldrich. Anhydrous *N*,*N*-dimethylacetamide (DMAc; puriss.) was obtained from Fluka, anhydrous dimethyl sulfoxide (DMSO; 99.7% pure) was from Acros Organics, hydrochloric acid (37%) was from J.T. Baker, lithium chloride (puriss. p.a., anhydrous) was from Fluka, and tetrahydrofuran (THF; analytical reagent) was from Riedel de Haën. Deionized water with a resistivity of 18.2 MΩ·cm was furnished by a Millipore system (Simplicity) fed with distilled water. Filter paper from Whatman International, which contains high-purity cellulose fibers, was used here.

In preparation of the TMSC derivative, to enable cellulose dissolution on anhydrous DMAc/LiCl, the fibers were first treated with 10 wt % aqueous NaOH solution at 80 °C for 1 h, washed three times with deionized water, and extracted twice in methanol and then in DMAc. A 1 g sample of cellulose fibers was then introduced to anhydrous DMAc containing LiCl (8 wt %) and kept under magnetic stirring at 130 °C for 1 h and finally at 100 °C for 2 h. After the mixture was allowed to stand at room temperature for 24 h, a translucent viscous solution was obtained. Cellulose was then derivatized by adding 10 mL of hexamethyldisilazane to 100 mL of the ensuing cellulose solution and heating at 80 °C for 1 h. After the separation by precipitation in ethanol and centrifugation at 2500 rpm for 15 min, TMSC was dissolved in THF. The concentration of the TMSC solution was about 500 mg/L.

Substrates of different dimensions, degreased using acetone and ethanol (anhydric and analytical grade from SDS) without further purification, were etched with a 1% solution of hydrofluoric acid following a procedure described elsewhere.[16] The samples were then totally covered by the TMSC solution and immediately spin-coated using speeds of 2000 and 5000 rpm for 60 s and an acceleration of 400 and 500 rpm/s, respectively. TMSC films were then regenerated by exposing them to HCl vapor for 20 s followed by argon flushing for 30 s.

The concentrations of the PI, MDI, and 4-bromoaniline solutions in anhydrous DMSO were on the order of 10^{-2} M.

Apparatus. An APT spin-coating machine was used for the deposition of the TMSC films.

ATR/MIR elements (800 μm thick) of undoped GaAs(100), covered by cellulose spin-coated films, were used as samples. Major faces of the ATR/MIR elements were cut in 40 mm × 15 mm rectangles and optically polished in 45° beveled edges in an isosceles trapezoidal configuration. This enables the transmitted infrared beam to be internally reflected about 25 times on each side of the element. ATR/MIR spectra were recorded using an FTIRS spectrometer (Magna-IR Nicolet 860) equipped with an MCT detector. The spectral resolution was 4 cm^{-1}. The kinetics of the interaction was obtained in situ. For this purpose, ATR/MIR spectra were recorded along the interaction using a homemade Teflon liquid cell provided with a hole for the introduction and extraction of the solution. Immediately after dissolution, the isocyanate solution was rapidly introduced into the ATR/MIR cell using a syringe. Then, a background spectrum was immediately recorded. The spectra were automatically recorded using a macro menu previously customized, enabling spectrum acquisition at preset conditions and a preset time. Following this procedure, one can ensure that positive (negative) peaks appearing in the spectra are due to species appearing (vanishing) either on the surface region or in the neighbor interphase cellulose solution. Between interactions with different solutions, intermediary rinses of the sample were accomplished, and a spectrum of the final washed film was recorded.

The XPS spectrometer used was an XSAM800 (Kratos) operated in the fixed analyzer transmission (FAT) mode, with a pass energy of 20 eV. The nonmonochromatized Mg Kα and Al Kα X-radiations ($h\nu$ = 1253.7 and 1486.7 eV, respectively) were produced using a current of 10 mA and a voltage of 12 kV. The samples were analyzed in an ultra-high-vacuum (UHV) chamber ($\sim 10^{-7}$ Pa) at room temperature, using 0° and 60° analysis angles relative to the normal to the surface. The spectra were recorded by a Sun SPARC Station 4 with Vision software (Kratos) using a step of 0.1 eV. A Shirley background was

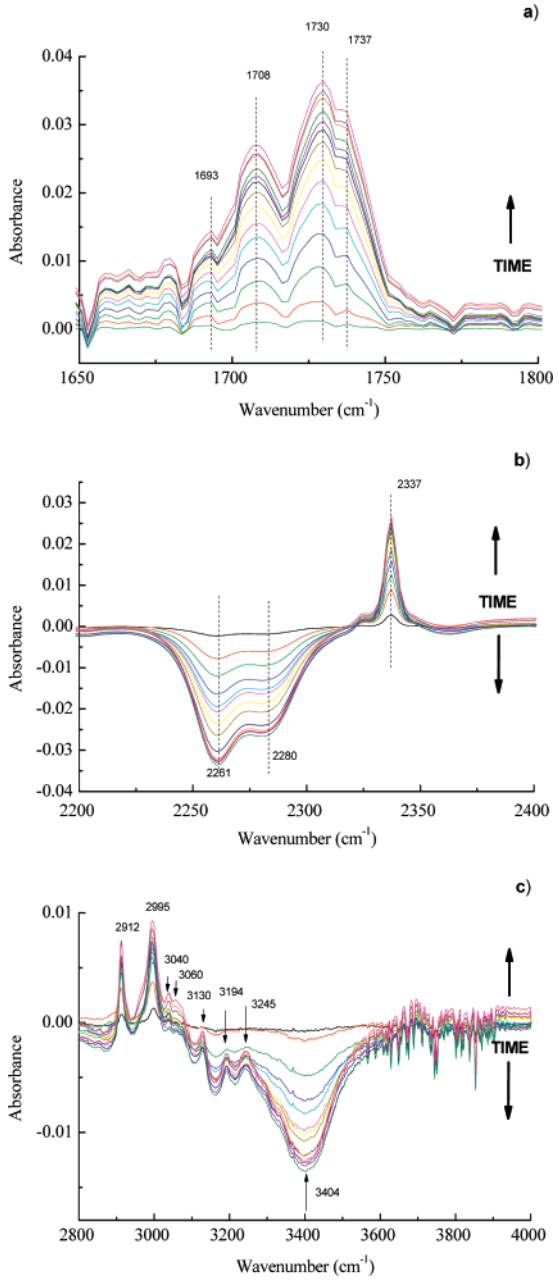

Figure 4. Three detailed regions of the survey spectra of Figure 3.

subtracted, and curve fitting for component peaks was carried out using Gaussian−Lorentzian products. No charge compensation (flood gun) was used. The binding energies were corrected using as a reference the binding energy of aliphatic carbon at 285 eV.[17,18] X-ray source satellites were subtracted. For quantification purposes, the sensitivity factors were 0.66 for O 1s, 0.25 for C 1s, 6.3 for As 2p, 4.74 for Ga 2p, 0.53 for As 3d, 0.31 for Ga 3d, and 0.42 for N 1s.

A Leybold-Heraeus ELS-22 spectrometer described before[19] was used for recording the HREELS spectra under a vacuum of $\sim 10^{-8}$ Pa. The incidence and analysis angles were in off-specular geometry, which is the adequate geometry for the impact regime enabling the analysis of a depth around 1 nm. The samples were carried to the UHV chamber under argon and introduced under a flux of pure nitrogen.

Results and Discussion

Cellulose Films. Thin films of silylated cellulose were spin-coated on GaAs(100) surfaces and regenerated by exposing them

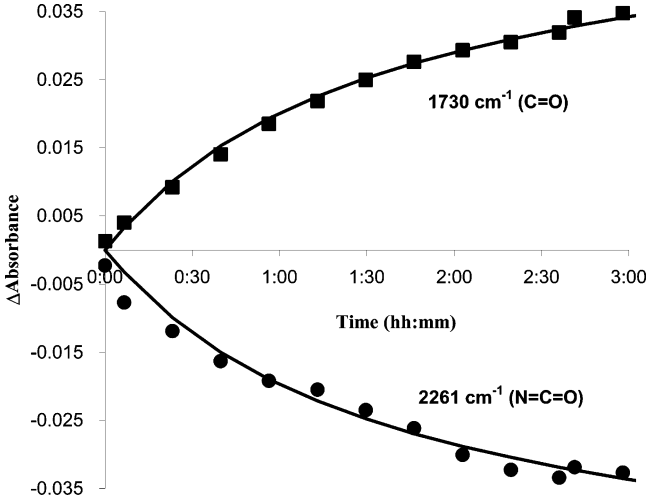

Figure 5. Evolution of the absorbance of C═O (1730 cm^{-1}) and N═C═O (2261 cm^{-1}) vibration modes along the PI reaction with cellulose. Full lines are fitted using eq 5.

to vapors of HCl. Figure 1 compares the ATR/MIR spectra of a TMSC spin-coated film before (A) and after (B) hydrolysis by exposition to HCl vapors with the transmission spectrum of crystalline cellulose (Avicel) dispersed in a KBr pellet (C).

Figure 1 shows that spectrum A of the silylated film is dominated by very intense peaks due to the presence of methoxy groups, namely, those of the silylated groups, the strong peaks corresponding to Si−C at 841 cm^{-1} and Si−O−C at 1041 cm^{-1}, respectively, and the bands of the methyl groups at 2880 and 2956 cm^{-1}. Another very characteristic peak found in this spectrum is the sharp band at 1250 cm^{-1} assigned to the symmetric deformation of methyl groups attached to silicon atoms. Major features appearing in spectra A, B, and C are assigned in Table 1 to the different vibrational modes.[20−23] The features appearing in the spectrum of the TMSC film decrease significantly after the exposition of the film to HCl vapors, giving rise to the characteristic peaks of cellulose, namely, those at 1021, 1067, and 1422 cm^{-1}. This confirms the regeneration of the cellulose film by HCl hydrolysis. The hydrophilicity change is also proved through two broad bands, centered at 1645 and 3340 cm^{-1}, characteristic of hydroxyl groups in interaction and some adsorbed water on the regenerated film surface. As a matter of fact, spectrum B of the regenerated cellulose is quite similar to the transmission spectrum of Avicel dispersed in a KBr pellet. Here, the band corresponding to the cellulose fibers appears to be broader, revealing the well-known intra- and interchain interactions through the OH groups, as was mentioned above. Taking into account the results of Carrillo,[24] the absence of a peak located at 895 cm^{-1} and the occurrence of one at 1422 cm^{-1} in spectrum B indicate some crystallinity of the regenerated film.

The presence of adsorbed water on the film is confirmed by the comparison of the ATR/MIR spectrum (already shown in Figure 1) and an HREELS (bold line) spectrum of a regenerated cellulose film deposited on GaAs (see Figure 2). The HREELS spectrum was recorded using incident electrons of 2.5 eV, an angle of incidence of 60°, and an angle of diffusion of 30°. As can be observed, introducing the film in a UHV system forces the adsorbed water molecules to be practically pumped from the surface. One can see that the broad bands present in the ATR/MIR spectrum at 1639 and around 3325 cm^{-1} practically disappear in the HREELS spectrum. In this off-specular geometry, analyzed electrons mainly result from impact interactions produced at short range and therefore mainly backscattered

SCHEME 1: Reaction of PI with the Cellulose Chains

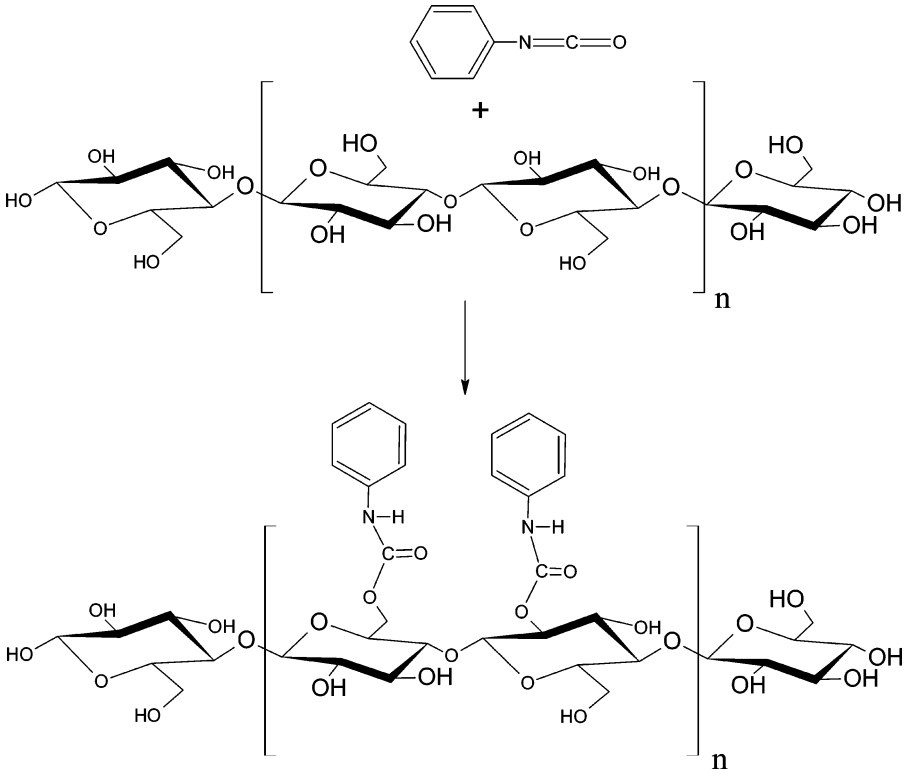

from the extreme surface of the film.[25] Except the water bands, in the HREELS spectrum all other bands are compatible with those observed by ATR/MIR corresponding to the whole thickness of the cellulose film. One can also note in the HREELS spectrum the absence of the CH_3 and the presence of the CH_2 stretching band assigned to the methylene groups at 1421 and 2884 cm^{-1}. Besides the characteristic peaks of cellulose, another typical peak at 290 cm^{-1}, assigned to the surface phonons of GaAs(100),[26] is observed. The existence of this peak is consistent with the presence of an ultrathin film on the GaAs substrate.

Interaction with PI. Figure 3 shows a set of survey ATR/MIR spectra recorded in situ during the interaction of cellulose with a solution of PI in DMSO. As the reference spectrum is recorded immediately after introduction of the solution into the cell, positive and negative peaks in the different spectra correspond to the appearance and disappearance of chemical species, respectively.

The most important negative bands are a narrow band centered at 2261 cm^{-1} corresponding to the isocyanate group (N═C═O) and a broad band (OH) centered at 3400 cm^{-1}. These bands correspond to species that disappear during the interaction, giving rise to new bonds at the interface with the cellulose film. Some OH groups in the surface region of the film are requested for the PI reaction. On the other hand, one can observe that all spectra exhibit several positive peaks corresponding to the formation of new species such as the aryl urethane groups on the cellulose surface, namely, the strong peak located at 1730 cm^{-1} assigned to the C═O stretching vibration and those at 1546 and 1508 cm^{-1} attributed to NH in-plane bending modes corresponding to the formation of the phenyl carbamate. The evolution of these bands is, as expected, followed by an increase of the intensity of the peak centered at 1601 cm^{-1} assigned to C═C stretching modes in the PI benzenic ring, which also attests the presence of the molecule at the surface.

The positive bands arising at 958 cm^{-1} (CH_3 rocking), 1313 and 1448 cm^{-1} (symmetric and asymmetric CH_3 deformation), and 2912 and 2995 cm^{-1} ($S-CH_3$ stretching modes) are characteristic of DMSO and confirm a certain penetration of the solvent in the cellulose film, i.e., the swelling of the film by the solvent. In fact, the OH groups are at the origin of the insolubility of the film, mostly in the case of solvents that do not form hydrogen bonds. As OH groups are consumed at the film surface, the solvent can more easily penetrate among the chains swelling, as referred, the cellulose film.

One should also note some intensity decrease of the broad band located at 1055 cm^{-1}, which can be ascribed to a light disentanglement of the cellulose chains, as a consequence of the functionalization of the film. However, this does not seem to affect the rest of the spectrum.

Different regions are detailed in Figure 4. Besides the peak appearing at 1730 cm^{-1}, one can see in more detail (Figure 4a) different components in the same band, namely, at 1708 and 1693 cm^{-1} corresponding to strong hydrogen bonding.[21] We relate the existence of these different components to urethane groups with dissimilar surroundings and therefore submitted to different constraints. This band can also include a contribution due to the PI molecules associated with neighbor unreacted OH groups in the cellulose fiber. The appearance of a band of increasing intensity with different components at 1693, 1708, 1730, and 1737 cm^{-1} confirms the grafting of the phenyl isocyanate to the cellulose, through its hydroxyl groups, with the formation of phenylcarbamate. On the other hand, Figure 4b shows that there is an enhancement of the negative bands characteristic of the isocyanate stretching vibration and most particularly those situated at 2261 and 2280 cm^{-1}. The presence of a narrow positive band at 2337 cm^{-1} with increasing intensity may reveal the presence of bound CO_2 species originated from the reaction of the remaining water molecules with isocyanate.[27] In the OH stretching region (Figure 4c), the decrease in intensity of the large band centered at 3400 cm^{-1} reveals some consump-

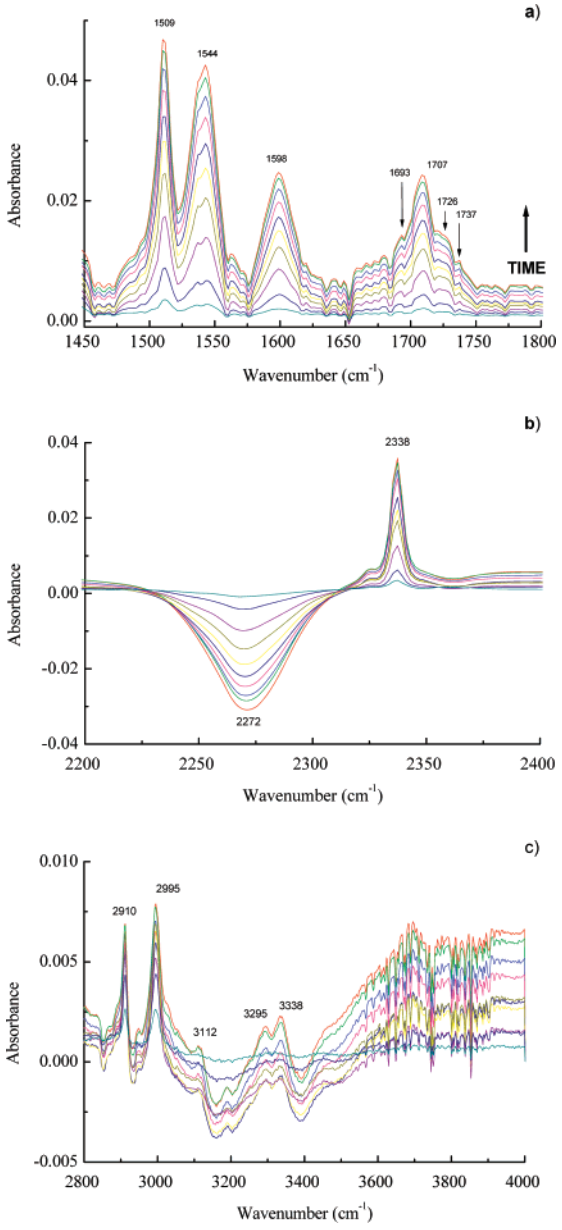

Figure 6. Detailed regions of the ATR/MIR spectra of a cellulose regenerated film in interaction with a solution of MDI in DMSO recorded in situ at different times after the background recording.

tion of hydroxyl groups of the cellulose film. This negative broad band partially hides the rise of the NH stretching positive bands of the carbamate groups located at 3130, 3194, and 3245 cm^{-1}. Still in this region, it is possible to see two weak peaks appearing at 3040 and 3060 cm^{-1} assigned to the CH stretching modes of the aromatic CH groups. No negative peaks corresponding to the cellulose absorbance were observed.

All these observations tend to confirm an efficient reaction of PI at the surface region of the film, proposed in Scheme 1, indicating the formation of phenylcarbamate groups appended to the cellulose surface, keeping the cellulose film integrity. Moreover, the different peaks related to carbamate function are still present even after washing of the film with pure DMSO, showing that PI molecules reacted with the surface.

The kinetics of the chemisorption of PI on the cellulose surface can be described in terms of the evolution of the absorbance of the bands at 1730 and 2261 cm^{-1}, as represented in Figure 5. The increasing intensity of the arising band corresponding to the appearance of carbonyl groups is accompanied by a clear decrease of the N═C═O band attesting the chemisorption of the isocyanate on the cellulose surface according to Scheme 1.

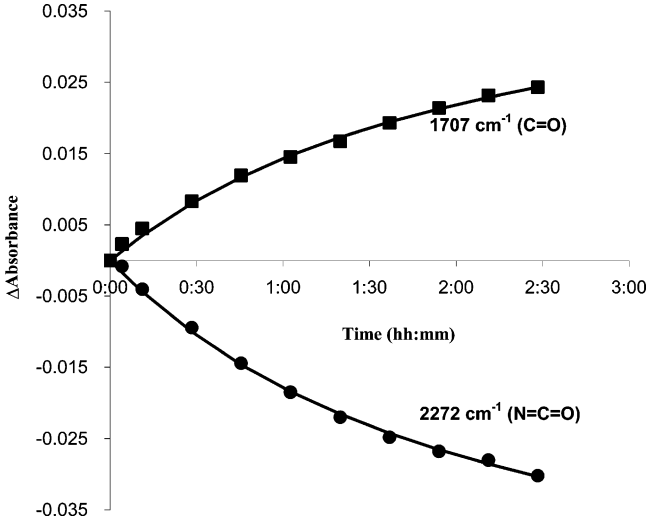

Figure 7. Evolution of the absorbance of C═O (1707 cm^{-1}) and N═C═O (2272 cm^{-1}) (squares and circles, respectively) stretching modes during the interaction of the cellulose film with a solution of 4,4′-methylenebis(phenylisocyanate) in DMSO. Full lines are fitted using eq 5.

One can consider for one type of alcohol function present at the surface of the cellulose film, the primary alcohols for instance, that

$$-\frac{dn_{1u}(t)}{dt} = k_1[n_{1u}(t)][PI] \quad (1)$$

where n_{1u} is the number of primary unreacted alcohols, [PI] is the isocyanate concentration, and k_1 is the rate constant. Assuming that the number of reacted PI molecules is negligible compared to the total number of PI molecules in solution, the integration leads to

$$n_{1u}(t) = n_{1u}(0)\exp(-k_1[PI]t) \quad (2)$$

$$n_{1r}(t) = n_{1u}(0) - n_{1u}(t) = n_{1u}(0)(1 - \exp(-k_1[PI]t)) \quad (3)$$

n_{1r} being the number of sites of primary alcohols that reacted.

Similarly, for secondary alcohols, one has

$$n_{2r}(t) = n_{2u}(0) - n_{2u}(t) = n_{2u}(0)(1 - \exp(-k_2[PI]t)) \quad (4)$$

n_{2r} and n_{2u} being the number of sites of secondary alcohols reacted and unreacted, respectively, with $n_{2u}(0) = 2n_{1u}(0)$.

Since the number of reacted PI molecules should be the same as the number of reacted hydroxyl groups, no matter the type, and the absorbance variation, ΔA, is proportional to the number of reacted PI molecules, we should have

$$-\Delta A_{PI}(t) \propto \Delta A_{CO}(t) \propto 1 - \exp(-k_1[PI]t) + 2(1 - \exp(-k_2[PI]t)) = 3 - \exp(-k_1[PI]t) - 2\exp(-k_2[PI]t) \quad (5)$$

In fact, the experimental data are perfectly fitted using eq 5, i.e. the sum of two exponential equations corresponding to the reaction of PI with the primary and the secondary alcohols. The characteristic times for the reaction of the primary and the secondary alcohols with the isocyanate group, $1/(k_1[PI])$ and $1/(k_2[PI])$, extracted from the fitting, give the values 43 and 230

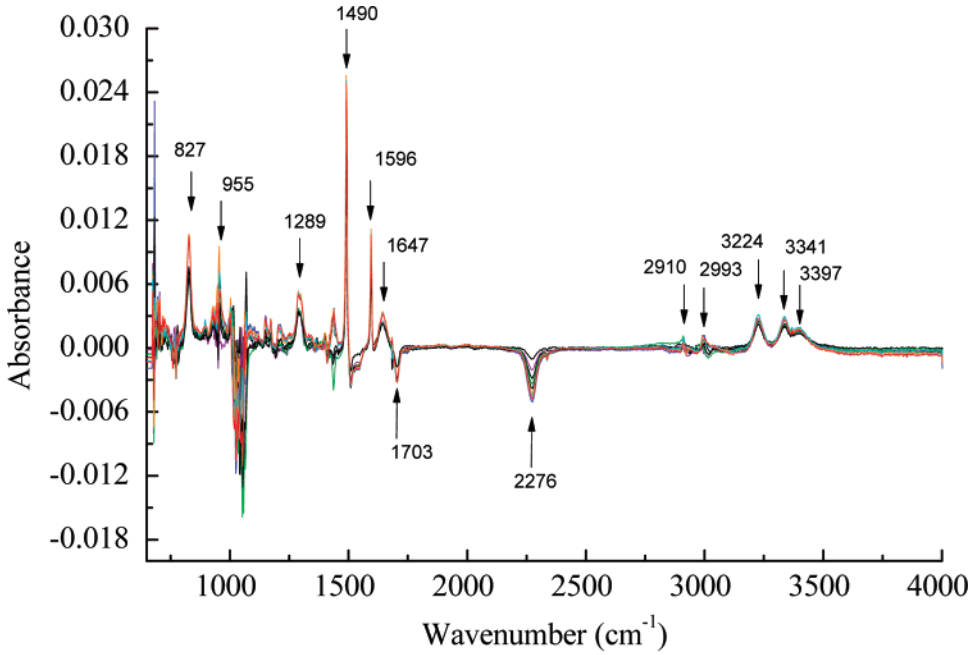

Figure 8. ATR/MIR spectra of a cellulose regenerated film previously treated with a solution of MDI in interaction with a solution of 4-bromoaniline in DMSO.

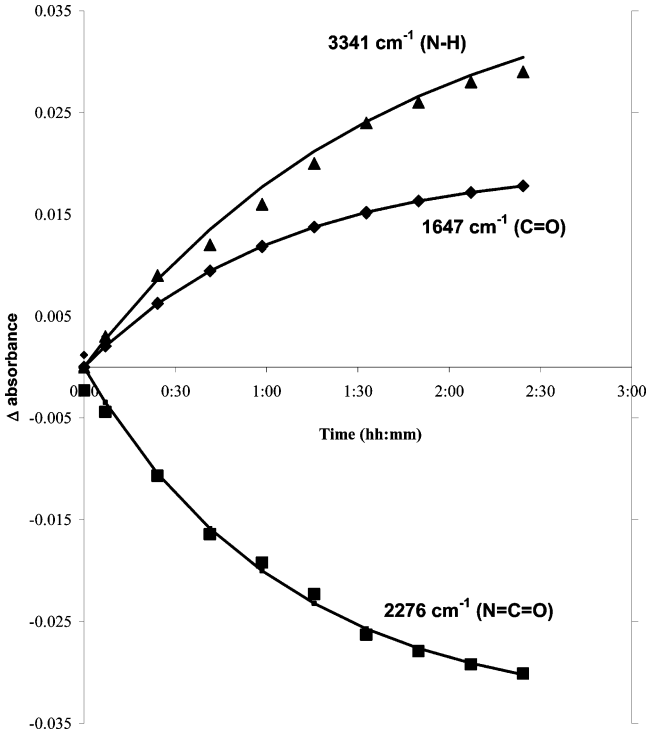

Figure 9. Evolution of the absorbance of the C═O vibration mode at 1647 cm^{-1} (◆), the N═C═O vibration mode at 2276 cm^{-1} (■), and the NH vibration mode at 3341 cm^{-1} (▲) during the interaction of a regenerated cellulose film previously treated with a solution of MDI with 4- bromoaniline.

min, respectively. Actually, primary alcohols are known to be more reactive than the secondary ones, the reactivity ratio primary/secondary alcohols varying with a factor from 6 to 10.[28] Using the least-squares method to optimize the curve fitting, the ratio of the constant rates estimated was $k_1/k_2 = 5.4 \pm 1.0$, which fully agrees, within the experimental error, with the reactivity ratio between primary and secondary alcohols. Concerning the absolute value of k_1, an assumption is needed to ascribe it a value: that the local concentration of phenyl isocyanate, [PI], be the same as the average concentration. Since this last one was $\sim 10^{-2}$ mol L^{-1}, $k_1 \approx 2.3$ mol^{-1} L min^{-1}. To our knowledge, the kinetic rate for the reaction of PI with cellulose in a homogeneous or heterogeneous medium was never measured. The kinetics of PI with alcohols was studied by several authors, and in particular, results were collected in a review by Caraculacu et al.[29] They show that the value of the rate constant increases with the alcohol concentration and with the existence of intramolecular hydrogen bonding in the alcohol. For instance, in very diluted solutions in benzene, 1,4-butanediol reacts with PI with a rate constant of 0.1216 mol^{-1} L min^{-1} when present in a concentration of 0.0438 mol L^{-1} and with a constant of 0.264 mol^{-1} L min^{-1} when present in a concentration of 0.0876 mol L^{-1}. The order of magnitude found for the reaction with the primary alcohols of cellulose given its local concentration at the surface then seems reliable.

Interaction with MDI. Diisocyanates are particularly interesting molecules as they can be envisaged as a link to chemisorb further functions, for instance, amines. In fact, as one of the isocyanate functions reacts with the hydroxyl groups exposed on the cellulose film, the opposite remains free and can subsequently be used to chemisorb an amine group, leading to an extended functionalization of the cellulose surface.

ATR/MIR spectra were also recorded during the interaction of a regenerated cellulose film with a solution of MDI in DMSO following in situ the evolution of the surface modification. Here again all spectra exhibit positive and negative peaks corresponding to the appearance and disappearance of chemical species, respectively. This reaction is quite similar to that previously described above using phenyl isocyanate. In fact, the maxima of most bands are found in neighboring positions of those found in the spectra presented in Figure 3. The spectra also reveal, as in the case of PI in DMSO, a small amount of solvent is trapped in the film.

Detailed spectral regions of the MDI kinetics are given in Figure 6. Figure 6a details the spectral region between 1450 and 1800 cm^{-1}. Positive peaks at 1707 and 1509 cm^{-1} correspond to the carbonyl and the amide groups, respectively. The fact that the maximum of the C═O band is shifted toward lower energies than in the PI spectra indicates that this group

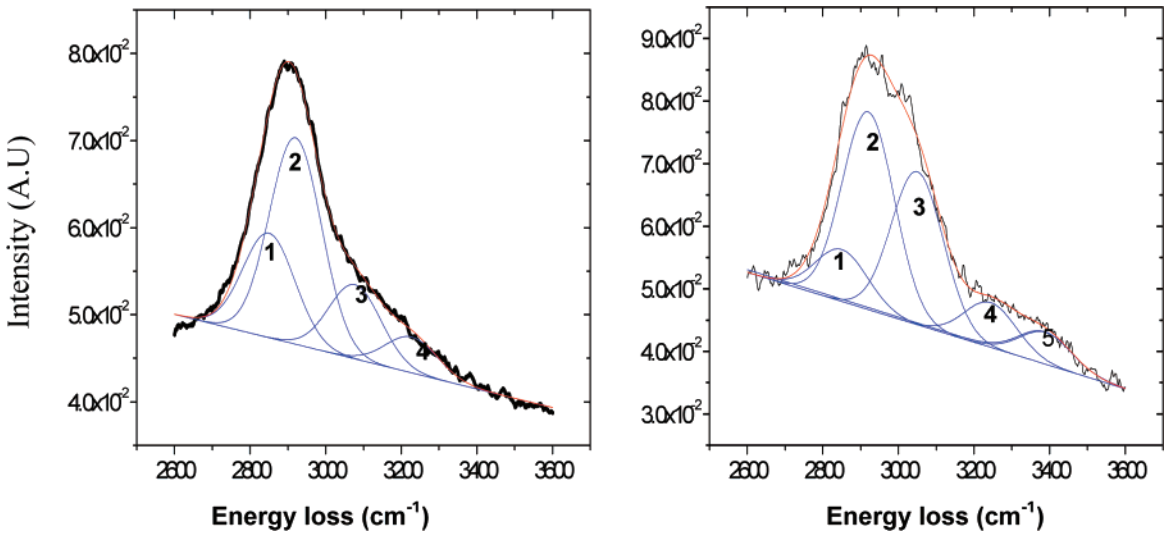

Figure 10. Comparison of the HREELS spectra of a regenerated cellulose sample before (left) and after (right) MDI/Br treatment in the domain of the CH stretching vibration modes. The spectra were recorded in the impact geometry using an angle of incidence of 60°, an angle of diffusion of 30°, and 3.5 eV incident electrons.

undergoes stronger interactions through hydrogen bonding than in the PI reaction. Also this band contains different components, the most important located at 1693, 1707, 1726, and at 1737 cm^{-1}, indicating different neighbors. This can also be explained by the larger volume associated with the MDI molecules. As in the PI reaction, in Figure 6b a negative band appears at 2272 cm^{-1}, assigned to the isocyanate extremity, which reacts with the cellulose film (vide Figure 6b). Also here, a very narrow positive band at 2338 cm^{-1} growing during the interaction reveals the presence of bound CO_2 species likely originated from the reaction of the remaining water molecules with isocyanate. The decrease of the band intensity confirms the consumption of a part of the isocyanate group in the reaction at the cellulose surface. Figure 6c clearly shows a broad negative OH band also, indicating the hydroxyl group consumption during the interaction. Here, one can also distinguish that positive peaks, corresponding to CH stretching of the solvent at 2910 and 2995 cm^{-1} and NH stretching modes at 3112, 3295, and 3338 cm^{-1} are superposed to the hydroxyl band.

As above, Figure 7 shows the evolution of the stretching modes of C═O (1707 cm^{-1}) and N═C═O (2272 cm^{-1}) during the interaction of a regenerated cellulose film with a solution of MDI in DMSO. As for PI, the band corresponding to carbonyl groups increases as the peak corresponding to the isocyanate function decreases, showing the consumption of the isocyanate group and the formation of the carbamate link with cellulose. The fitting of the experimental data is outstandingly good when the sum of two exponential equations (eq 5) for the primary and secondary alcohols is used. The extrapolated characteristic times for the primary and secondary hydroxyl reaction, $1/(k_1[MDI])$ and $1/(k_2[MDI])$, with the isocyanate group resulting from this fitting are now 61 and 396 min, respectively. The ratio of the constant rates found for MDI is $k_1/k_2 = 6.4 \pm 1$, which also fully agrees, within the experimental error, with the relative reactivity ratio for PI, given above. The increase of k_1/k_2 can be explained by the fact that in this case there are two isocyanate extremities, instead of one in the case of PI.

Figure 8 shows a set of ATR/MIR spectra following the kinetics of a cellulose film modified by MDI in interaction with a 10^{-2} M solution of 4-bromoaniline in DMSO. As before, one can also note a slight penetration of the solvent in the surface region of the film, attested by the positive bands at 2910 and 2993 cm^{-1} assigned to stretching modes of S−CH_3 of DMSO. Here the negative peak at 2276 cm^{-1}, revealing the consumption of N═C═O during the reaction, is quite remarkable. This attests the involvement of the reactive extremity of MDI on the reaction with the 4-bromoaniline molecules. The band centered at 1490 cm^{-1} in all spectra indicates the presence of a urea group and is assigned to the symmetric stretching vibration of N−C−N.[21] The peak at 1596 cm^{-1} is assigned to the NH deformation. Both peaks are intense and very narrow, suggesting the absence of intramolecular interactions. However, the band due to the stretching vibration of C═O appearing at 1647 cm^{-1} is broader, which can be explained by different contributions of the carbonyl groups in the grafted entity. A negative peak at 1703 cm^{-1} also shows the modification of the C═O bond during the interaction. In the region between 3000 and 4000 cm^{-1}, besides the appearance of the three bands at 3224, 3341, and 3397 cm^{-1}, characteristic of the NH stretching modes, no OH band appears. This confirms that no hydroxyl groups are involved in the reaction.

Here, the kinetics of the film modification follows a single-exponential adsorption law ($\Delta A \propto 1 - \exp(-t/\tau)$). In Figure 9, the intensity of the bands centered at 1647 and 3341 cm^{-1} corresponding to C═O and N−H is represented vs time. The negative intensity corresponding to the band at 2276 cm^{-1} points out the disappearance of the isocyanate groups, consumed during the reaction. All the curves were best fitted with the same characteristic time, $\tau = 66$ min.

A sample prepared following this kinetics was analyzed by HREELS in the impact regime. The electron energy loss domain of CH stretching is presented in Figure 10. Comparison of the spectra of a regenerated cellulose film before and after interaction with MDI followed by that of 4-bromoaniline confirms the presence of the phenyl groups at the extreme surface of the cellulose film. In fact, in the second case, besides the components corresponding to stretching vibrations of the aliphatic CH (1 and 2), a much stronger component (3) at 3050 cm^{-1} characteristic of the aromatic CH and a new one (5) at 3390 cm^{-1}, assigned to NH stretching modes, appear. Component 4 is assigned to a multiple loss, most likely that of a CH stretching combined with a GaAs phonon. The high sensitivity of HREELS in the impact configuration to the extreme surface of the film

SCHEME 2: Reaction of Cellulose Chains with MDI Followed by the Reaction with 4-bromoaniline

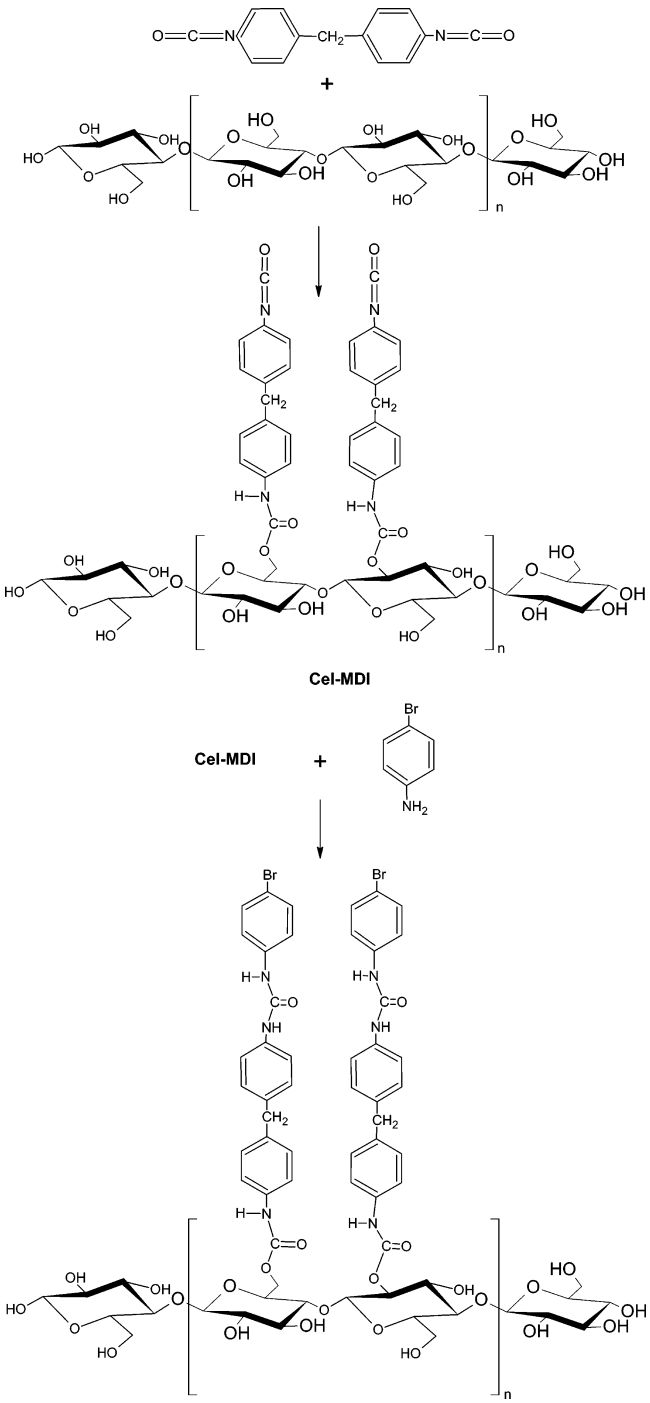

is less than 1 nm, confirming the presence of aromatic rings in the added pendant groups on the surface after reaction.

From these results the chemical reaction representative of the modification of the cellulose surface is proposed in Scheme 2. The scheme proposed indicates two possible sites corresponding to the primary and secondary alcohols.

The presence of the pendant groups presented in Scheme 2 totally agrees with the XPS analysis presented in Figure 11. Four XPS regions are exhibited. The (a) carbon (C 1s), (b) oxygen (O 1s), and (c) nitrogen (N 1s) regions, for two cellulose surfaces, one modified by PI and another modified by MDI followed by the interaction with 4-bromoaniline, are compared (denoted by MDI/BrA in the figure). The (d) bromine region (Br 3p) only concerns the cellulose film modified by MDI followed by the interaction with 4-bromoaniline. Table 2[14−16,30,31] presents the assignments of the peaks of Figure 11.

C 1s regions of the XPS spectra of cellulose samples derivatized with isocyanates are fitted with six components. C 1s 1, centered at 284.6 eV, is attributed to phenyl group aromatic CH. C 1s 2, centered at 285 eV, corresponds to aliphatic CH. C 1s 3, centered at 285.8 eV, is mainly assigned to carbon of the phenyl groups bound to nitrogen of the isocyanate groups, C−N. However, in the spectrum of the MDI/BrA sample, this peak can also include other contributions of the grafted 4-bromoaniline: C−Br and C−NH_2 (see Table 2). C 1s 4, at 286.7 eV, is assigned to C−O of cellulose, and C 1s 5, at 288.1 eV, is attributed to O−C−O of cellulose. Finally, C 1s 6, at ∼289 eV, is assigned to O−C═O in bound phenyl isocyanates and to N−(C═O)−N in bound bromoaniline. As expected, the relative intensities of C 1s 4 and C 1s 5 (cellulose peaks) are higher in PI than in MDI/BrA, the atomic ratio cellulose/NCO being 3.4 in PI and 1.4 in MDI/BrA. This result shows that, in this case, the cellulose signal is more attenuated than in the PI case. The bromine doublet, separated by 6.7 eV, is clearly detected in the modified surface as shown in Figure 11d. However, the low amount of Br does not allow a sound quantification. In the O 1s region, the main component (O 1s 1), centered at 531.3 ± 0.2 eV, corresponds to the substrate oxides. In the MDI/BrA spectrum this peak can also include the contribution of bound bromoaniline, N(CO)N, reported in the literature at 531.41 eV. O 1s 2, at 532.8 ± 0.1 eV, includes several contributions from the oxygen present in the adsorbed organic layer, namely, the oxygen atoms from the glucopyranose ring of cellulose and those from O−C═O, which were not possible to resolve. N 1s is fitted with just one component centered at 400.2 ± 0.2 eV, assigned to N(CO)N in MDI/BrA and to $NHCOO^-$, in agreement with the bound phenyl isocyanate (carbamate). The N 1s region of the MDI/BrA spectrum has a full width at half-maximum (fwhm) larger (2.5 eV) than that of the PI spectrum (2.1 eV), since it includes the contribution of amine groups.

The thicknesses of modified cellulose layers adsorbed onto GaAs substrates were estimated using the quantitative XPS results. The GaAs substrates of the cellulose films submitted to different etching treatments have already been characterized.[16] XPS spectra recorded with derivatized cellulosic films deposited on GaAs show clearly the Ga and As XPS regions, indicating the existence of a very thin organic layer, less than 10 nm thick, or of a layer containing holes. The evaluation of the film thickness was based on the XPS atomic ratios for two different anodes (Mg Kα and Al Kα) and two different analysis angles for each (0° and 60° relative to the normal to the surface). Two different models were tested: a homogeneous continuous layer of constant thickness and an islandlike layer.[32] For the first model, the fitted parameters were the atomic density ratios n_C/n_{Ga} (where n_C and n_{Ga} are, respectively, the carbon density in the film and the gallium density in the substrate) and the layer thickness. In the second model, also the coverage fraction was used. No good match between the experimental and fitted data could be obtained using the first method. Contrarily, with the second one, an average value of 1.1 for n_C/n_{Ga} was obtained, which is a reliable value, reasoning from the bulk densities of both the organic film and the GaAs substrate.[32]

Table 3 presents the values of the mean thickness and the covered surface fraction of different cellulose-based samples. The thickness and the covered fraction were estimated by fitting the islandlike model to the experimental XPS atomic ratios X/Ga and X/As (X being carbon and nitrogen).

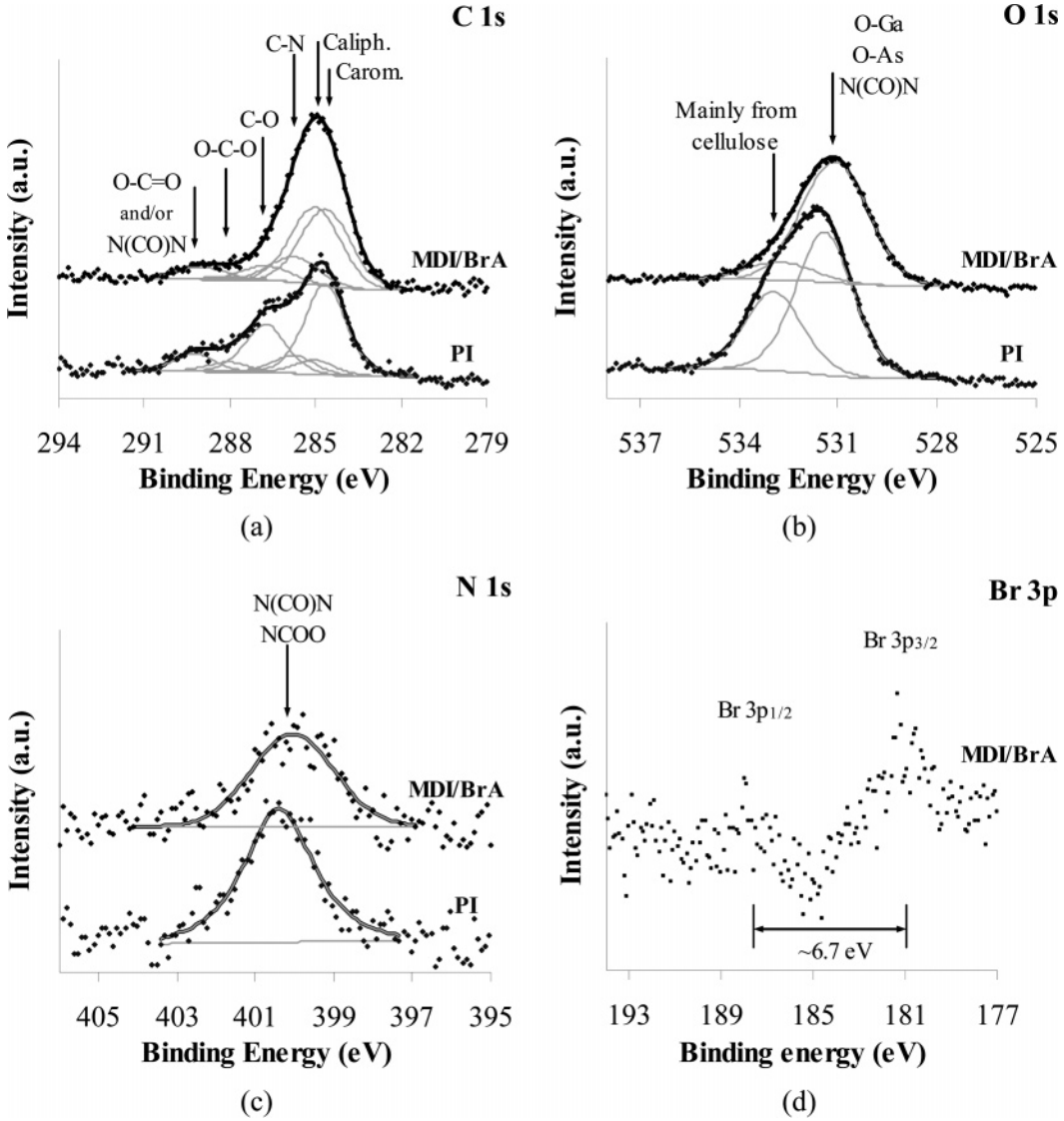

Figure 11. XPS regions (a) C 1s, (b) O 1s, (c) N 1s, and (d) Br 3p of cellulose samples treated with PI and MDI/BrA. The bromine region (Br 3p) (d) only concerns the MDI/BrA sample. C 1s, O 1s, and Br 3p were recorded using Al Kα radiation, and N 1s was recorded using Mg Kα radiation at a 0° angle of analysis.

TABLE 2: Assignments of Peaks Fitted in XPS Regions C 1s, O 1s, and N 1s of PI and MDI/BrA Samples[a]

	binding energy (eV)			
peak	PI	MDI/BrA	lit.[16,17,29,30]	assignment
C 1s 1	284.6	284.6	284.6	aromatic −CH
C 1s 2	285.0	285.0	285.0	aliphatic −CH
C 1s 3	285.8	285.8	285.74−285.94	C−N in phenyl isocyanate + C−Br and C−NH_2 in bromoaniline
C 1s 4	286.7	286.7	286.73	C−O in cellulose
C 1s 5	288.1	288.1	288.06	O−C−O in cellulose (note that C═O in free phenyl isocyanate is at 287.1−287.9 eV)
C 1s 6	289.2	289.0	288.84	−NCOO− in bound phenyl isocyanate
			289.6	+ −N(CO)N− in bound bromoaniline
O 1s 1	531.4	531.1	530.7−532.3	Ga_2O_3, As_2O_3
			531.41	−N(CO)N− in bound bromoaniline
O 1s 2	532.9	532.8	532.93 and 533.51	C−O in cellulose
			533.6	O−C═O
			399.89	−N(CO)N− in bound bromoaniline
N1s 1	400.4	400.1	400.32	−NCOO− in bound phenyl isocyanate (note that −NCO in free phenyl isocyanate is at 400.2 eV)

[a] The charge shift was corrected using as a reference the binding energy of aliphatic carbons at 285 eV. Numbered peaks correspond to fitted peaks from right to left.

It is interesting to notice that the thickness does not change substantially from TMSC to regenerated cellulose, but only slightly diminishes. This can be assigned to a higher compactness of the film due to the appearance of new hydrogen bonds after the hydrolysis or even a further crystallization, besides the replacement of methyl groups by hydroxyl ones. Also, when

TABLE 3: Estimated Thickness and Coverage Fraction of Different Cellulose Samples Obtained from XPS Data

	TMSC	cellulose (*R*)	PI	MDI/BrA
thickness (nm)	7.3 ± 0.2	6.8 ± 0.5	6.7 ± 0.1	9.1 ± 0.8
covered fraction ((0.02)	0.90	0.86	0.94	0.92

PI molecules react with the film, the thickness still remains quite constant. In fact, the molecular length of PI is not significant compared to the roughness of the film (~2.5 nm from measurements AFM), and PI can fill the valleys existing in the regenerated film or even be included in the cellulose ring. This is consistent with the fact that the covered fraction increases with the adsorption of PI. For the MDI/BrA sample the covered fraction is similar to that of the PI sample, but the mean thickness increases, in agreement with the length of the grafted molecular segments.

A representation of the grafted segment is given in Figure 12. Taking into account the bond angles and using the software ACD/3D, the molecular length of the grafted part was evaluated to be 2.4 nm. These results are in agreement with an effective reaction between MDI and the hydroxyl groups of the surface. They also suggest that the MDI segment grafted is stretched on the cellulose surface after the reaction of the first isocyanate group. This conformation is thermodynamically favored as it enables hydrogen bonding to be established between hydroxyl groups. On the other hand, such a conformation sets free the second NCO function for a posterior reaction, enabling a subsequent functionalization of the surface or even providing the possibility for creating further molecular architecture.

Another question that can be answered by the XPS results concerns the degree of substitution (DS). It is usually expressed as the number of hydroxyl groups substituted by ring, the maximum then being 3. In the C 1s region, we have a peak corresponding to C−O bonds and another to the urethane group (NCOO), formed by the reaction of the isocyanate with the hydroxyl groups. The C−O peak corresponds to five C−O bonds by ring: 2 within the ring and 3 to alcohol groups, independently of being substituted or not. The urethane group measures the substituted alcohol groups. The following equation may then be used to estimate DS:

$$\mathrm{DS} = 3\frac{\mathrm{NCOO\ area}}{{}^{3}/_{5}(\mathrm{CO\ area})} = 5\frac{\mathrm{NCOO\ area}}{\mathrm{CO\ area}} \qquad (6)$$

Obviously, the value reached is, in principle, a maximum one because the signal coming from more superficial groups is less attenuated than the signal coming from deeper species. For the PI/cellulose samples, the value of the thickness and covered fraction suggests that PI is not in the form of a layer on the cellulose but rather within pores. Equation 6 should then be applicable, and the value found for DS should be close to the real value. It gives 1.6 ± 0.2. However, for MDI, the results suggest a strong stratification of layers and eq 6 loses validity.

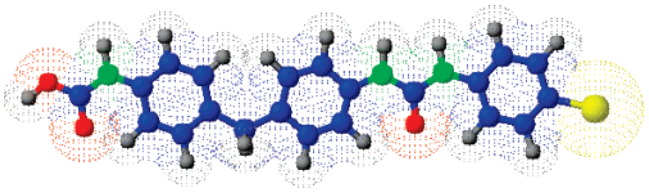

Figure 12. MDI molecule bound to a bromoaniline molecule scheme. Color code: blue, carbon; gray, hydrogen; green, nitrogen; yellow, bromine; red, oxygen. Drawn with ACD/3D software.

Conclusions

Cellulose films of nanometric dimensions were deposited on gallium arsenide surfaces from derivatized cellulose followed by regeneration through aqueous HCl vapors. These resulting cellulose films are very resistant to solvents. The different experiments performed in this study show that the films are also strongly attached to the substrate, likely due to van der Waals or hydrogen bonding. Even after 24 h of immersion in the solution, cellulose films do not detach from the GaAs substrate. This enables the kinetics of different molecules in solution to be followed for periods of several hours. During interaction with the solution, films are only slightly swollen by the polar solvents used here. These facts could be observed in the ATR/MIR spectra progressively recorded. ATR/MIR was basically used in situ to follow the kinetics of interaction of the cellulose films with PI and MDI molecules. The spectra clearly show the formation of an increasing number of carbonyl and amine groups and the decrease of the hydroxyl groups, confirming the reaction of the isocyanate groups with the hydroxyl groups of the cellulose surface. Slight penetration of the solvent (DMSO) was also observed. The loss of cellulose after the reaction was insignificant. The study of the development of carbonyl and amino groups on the surface, during PI or MDI reaction, allowed the conclusion that both primary and secondary alcohols are consumed during the interaction with a rate ratio on the order of 6 ± 1, compatible with the well-known difference of reactivity of primary and secondary alcohols. A value of ~2 $\mathrm{mol^{-1}\ L\ min^{-1}}$ was obtained for the reaction of PI with the primary alcohols. MDI containing two isocyanate groups enables the use of the second group (not linked to the cellulose) to be posteriorly used. To test the possibility of creating new linked species on the surface, a bromoaniline was used after the MDI interaction. The kinetics show that bromoaniline promptly reacts with the isocyanate groups exposed at the surface. These results are in good agreement with HREELS and XPS data. HREELS confirms the presence of new aromatic groups at the extreme surface of the cellulose film. XPS also detects all the elements and new bonds of the different organic groups grafted to the cellulose surface. Furthermore, from XPS data, the thickness of the films could be estimated to be around 7 nm, with the fraction of the covered area of the different samples always attaining values near unity. We can conclude that this work opens new perspectives to the development of cellulose surfaces, mainly concerning the surface chemistry of this natural polymer. This point is especially interesting for the functionalization of cellulose surfaces and suggests new applications of cellulose when used as a substrate. This study also proves that the chemistry of cellulose already known in the homogeneous phase and the heterogeneous phase with cellulose fibers also persists in nanofilms deposed on semiconducting surfaces, keeping the integrity of the film. Finally, this study opens a novel way of achieving molecular architecture on cellulose films deposited on semiconductor surfaces following in situ the introduction of new chemical groups, especially those with recognizable properties.

Acknowledgment. We acknowledge NATO Project CBP-.MD.CLG982316, the bilateral cooperation of the Ministère de la RechercheF Scientifique, Technologique et de Développement des Compétences (Tunisia), with GRICES (Portugal), Grant TP/20065, Project DGRST/CNRS (France), Grant 06R 12-06, and the FCT for a postdoctoral grant (A.M.F.), SFRH/BPD/26239/2006, for financial support.

References and Notes

(1) Brodsky, M. H. *Sci. Am.* **1990**, *262* (2), 68−75.

(2) Ashkenasy, G.; Cahen, D.; Cohen, R.; Shanzer, A.; Vilan, A. *Acc. Chem. Res.* **2002**, *35*, 121−128.

(3) Rei Vilar, M.; El Beghdadi, J.; Debontridder, F.; Naaman, R.; Arbel, A.; Ferraria, A. M.; Botelho do Rego, A. M. *Mater. Sci. Eng., C* **2005**, *26*, 253−259.

(4) Harrick, N. J. *Internal Reflection Spectroscopy*; Interscience Publishers, John Wiley & Sons: New York, 1967.

(5) Schempp, W.; Krause, T.; Seifried, U.; Koura, A. *Das Papier* **1984**, *38*, 607−610.

(6) Schaub, M.; Wenz, G.; Wegner, G. *Adv. Mater.* **1993**, *5*, 919−922.

(7) Buchholz, V.; Wegner, G.; Stemme, S.; Ödberg, L. *Adv. Mater.* **1996**, *8*, 399−402.

(8) Kontturi, E.; Thune, P. C.; Niemantsverdiriet, J. W. *Polymer* **2003**, *44*, 3621−3625.

(9) Kontturi, E.; Thune, P. C.; Alexeev, A.; Niemantsverdiriet, J. W. *Polymer* **2005**, *46*, 3307−3317.

(10) Rojas, O. J.; Ernstsson, M.; Neuman, R. D.; Claesson, P. M. *J. Phys. Chem B* **2000**, *104* (43), 10032−10042.

(11) Österberg, M. *J. Colloid Interface Sci.* **2000**, *229*, 620−627.

(12) Botaro, V. R.; Gandini, A. *Cellulose* **1998**, *5*, 65−78.

(13) Williamson, S. L.; McCormick, C. L. *J. Macromol. Sci., Part A: Pure Appl. Chem.* **1998**, *35*, 1995−1927.

(14) Gandini A.; Botaro V.; Zeno E.; Bach S. *Polym. Int.* **2001**, *50*, 7-9.

(15) Heinze, T.; Liebert, T. *Prog. Polym. Sci.* **2001**, *26*, 1689−1762.

(16) Rei Vilar, M.; El Beghdadi, J.; Debontridder, F.; Artzi, R.; Naaman, R.; Ferraria, A. M.; Botelho do Rego, A. M. *Surf. Interface Anal.* **2005**, *37*, 673−682.

(17) Wagner, C. D.; Naumkin, A. V.; Kraut-Vass, A.; Allison, J. W.; Powell, C. J.; Rumble, J. R., Jr. NIST X-ray Photoelectron Spectroscopy Database, NIST Standard Reference Database 20, Version 3.4 (Web Version), http://srdata.nist.gov/xps/, 2003.

(18) Beamson, G.; Briggs, D. *High Resolution XPS of Organic Polymers. The Scienta ESCA300 Database*; John Wiley & Sons: New York, 1992.

(19) Rei Vilar, M.; Botelho do Rego, A. M.; Lopes da Silva, J.; Abel, F.; Schott, M.; Quillet, V.; Petitjean, S.; Jérôme, R. *Macromolecules* **1994**, *27*, (20), 5900−5906.

(20) Tsuboi, M. *J. Polym. Sci.* **1957**, *25*, 159−171.

(21) Zhbankov, R. G.; Firsov, S. P.; Buslov, D. K.; Nikonenko, N. A.; Marshewka, M. K.; Ratajczak, H. *J. Mol. Struct.* **2002**, *614*, 117−125.

(22) Carrillo, F.; Clom, X.; Suñol, J. J.; Saurina, J. *Eur. Polym. J.* **2004**, *40*, 2229−2234.

(23) Socrates, G. *Infrared Characteristic Group Frequencies*, 2nd ed.; Wiley International Publication; John Wiley & Sons: Chichester, U.K., 1994.

(24) Colom, X.; Carrillo, F. *Eur. Polym. J.* **2002**, *38*, 2225−2230.

(25) See for instance, Botelho do Rego, A. M.; Rei Vilar, M.; Lopes da Silva, J. *J. Electron Spectrosc. Relat. Phenom.* **1997**, *85*, 81−91.

(26) Dubois, L. H.; Schwartz, G. P. *J. Electron Spectrosc. Relat. Phenom.* **1983**, *29*, 175−180.

(27) McCowan C. S.; Caudle M. T. *Dalton Trans.* **2005**, (2), 238−246.

(28) Cheremisinoff, N. P. *Handbook of Polymer Science and Technology*; Marcel Dekker: New York, 1989.

(29) Caraculacu, A. A.; Coseri, S. *Prog. Polym. Sci.* **2001**, *26*, 799−851.

(30) Zhao, C. G.; Ji, L. J.; Liu, H. J.; Hu, G. J.; Zhang, S. M.; Yang, M. S.; Yang, Z. Z., *J. Solid State Chem.* **2004**, *177*, 4394−4398.

(31) Angellier, H.; Molina-Boisseau, S.; Belgacem, M. N.; Dufresne, A. *Langmuir* **2005**, *21*, 2425−2433.

(32) Botelho do Rego, A. M.; Ferraria, A. M.; El Beghdadi, J.; Debontridder, F.; Brogueira, P.; Naaman, R.; Rei Vilar, M. *Langmuir* **2005,** *21*, 8765−8773.